2019 International Conference on Robotics and Automation (ICRA)
Palais des congres de Montreal, Montreal, Canada, May 20-24, 2019

Tele-Echography using a Two-Layer Teleoperation Algorithm with Energy Scaling

Enrico Sartori[1], Carlo Tadiello[1], Cristian Secchi[2], Riccardo Muradore[1]

Abstract— **Performing ultrasound procedures from a remote site is a challenging task since both a stable behavior, for the safety of the patient, and a high-level of usability, to exploit the sonographer's expertise, need to be guaranteed. Furthermore, a teleoperation system that provides such requirements has to deal with communication delays as well. To address this issue, we use the two-layer algorithm: a passivity-based bilateral teleoperation architecture able to guarantee stability despite unknown and time-varying delay. Its flexibility allows to implement different kinds of control laws. In a Tele-Echography system, the slave manipulator has to apply significant forces needed by the procedure whereas the haptic device at the master side should be very light to avoid tiring the operator. Therefore, the energy needed by these two robots to perform their movements is very different and the energy injected into the system by the operator is often not sufficient to implement the desired action at the slave side. Methods to overcome this problem require to perfectly know the dynamical models of the robots. The solution proposed in this paper does not require such knowledge and is based on properly scaling the energy exchanged between the master and the slave side. We show the effectiveness of this approach in a real setup using a TOUCH haptic device and a WAM Barrett robot holding an ultrasound probe.**

I. INTRODUCTION

Ultrasound examination is a medical procedure widely used since it is inexpensive, non-ionizing and non-invasive. This procedure needs expert operators: the task is highly dependent on the anatomical regions and on the pathology to explore. Unfortunately, the availability on-site of skilled sonographers is not always possible, especially for remote or scarcely populated regions. Research activities over the years developed many teleoperated robotic solutions to allow medical experts to remotely perform such procedures. In the SYRTECH project [1], a system has been proposed to perform ultrasound examinations from a remote site by using a lightweight and portable device. Another interesting solution is TER [2], a tele-robotic system where the controller at the slave side is designed to split translational and rotational movements. Technical and clinical feasibility of the approach was provided in [3]. For recent results we refer the reader to [4] and the reference therein. A Tele-Echography architecture using only commercial device is discussed in [5]. In the above articles, the problem of system instability due to communication delay is not addressed since only high performance network (e.g ISDN, Integrated Services Digital Network) or dedicated communication channels are considered. Furthermore, several other factors can have a negative impact on the stability of bilateral teleoperation systems such us: 1) relaxed user grasping; 2) stiff position and force control settings; 3) hard contact with the remote environment, [6].

An elegant solution to prevent these factors from destabilizing the system is passivity-based control. Controlling the overall teleoperation system to make it behaves as a passive system allows to achieve a stable interaction with human operators [7] and passive environments [8].

Unfortunately, passivity usually leads to a reduction of the transparency level [9], [10], [11], [12], [13], [14], [15]. A different passive-based solution is the Two-Layer architecture proposed by Franken *et al.* [16] where stability and transparency are addressed in a seamless way by implementing a hierarchical two-layer approach.

When master and slave manipulators are mechanically identical, the amount of energy supplied to the system by the operator at the master side is the same needed by the slave robot to execute the corresponding motion. Problems arise when the robots are different because the energy consumption to perform the same action is very different. This behavior involves the draining of the energy tanks that is perceived by the passivity layer as a passivity loss. The damping injection proposed in [16] to harvest more energy from the user is not sufficient in this case: the overall teleoperation system becomes quickly unusable.

The contribution of this paper is a new version of the two-layer approach where it is possible to scale the energy exchanged between the master and the slave tanks. In this way, it will be possible to cope with the different energy needs of master and slave robots. We will show that the proposed scaling preserves the passive (and so stable) behavior of the overall teleoperation architecture.

This paper is organized as follow: in Section II we introduce the two-layer teleoperation architecture. In Section III we discuss the proposed energy scaling approach and we formally prove the passivity. In Section IV the experimental setup is described whereas in Section V experiment results are shown. Conclusions are drawn in Section VI.

This work has received funding from the European Union's Horizon 2020 research and innovation programme under grant agreement No. 779813 (SARAS project, www.saras-project.eu). This work was partly supported by the project MIUR "Department of Excellence" 2018-2022.

[1]Enrico Sartori, Carlo Tadiello and Riccardo Muradore are with the Altair Lab, Department of Computer Science, University of Verona. {enrico.sartori, carlo.tadiello, riccardo.muradore}@univr.it

[2]Cristian Secchi is with the ARSControl Lab, Department of Engineering Sciences and Methods, University of Modena and Reggio Emilia. cristian.secchi@unimore.it

Enrico Sartori and Carlo Tadiello contributed equally to this work.

II. Two-Layer Bilateral Teleoperation

Let

$$B_i(x_i)\ddot{x}_i + C_i(x_i,\dot{x}_i)\dot{x}_i + R_i(x_i)\dot{x}_i = F_i + F_i^{ext} \quad (1)$$

be the Euler-Lagrange model of the gravity compensated master and slave robots. The subscript $i = m, s$, denotes the side of the robot (master or slave), $x_i \in \mathbb{R}^6$ is the Cartesian pose of the robot, F_i is the control wrench, F_i^{ext} is the interaction wrench, in particular $F_m^{ext} = F_h$ (the force applied by the operator) and $F_s^{ext} = F_e$ (the reaction environment force). The term $B_i(x_i)$ is the inertia matrix, $C_i(x_i,\dot{x}_i)$ is the matrix of the centrifugal and Coriolis terms, and $R_i \geq 0$ is a positive semidefinite damping matrix representing friction and local damping injections [16].

Let $H_i(t) = \frac{1}{2}\dot{x}_i^T B_i(x_i)\dot{x}_i$ be the kinetic energy of the robot. Considering (1), it can be easily shown that

$$\dot{H}_i(t) = -\dot{x}_i^T R_i \dot{x}_i + \dot{x}_i^T(F_i + F_i^{ext}) \quad (2)$$

which yields the following power balance that proves the passivity of (1)

$$\dot{H}_i(t) \leq \dot{x}_i^T(F_i + F_i^{ext}). \quad (3)$$

For the tele-echography application, we implement a two-layer Position-Position teleoperation architecture shown in Figure 1. The control architecture is implemented within the upper *transparency layer*, whereas the bottom *passivity layer* monitors the energy flow among the different subsystems using two energy tanks (T_m at the master side and T_s at the slave side).

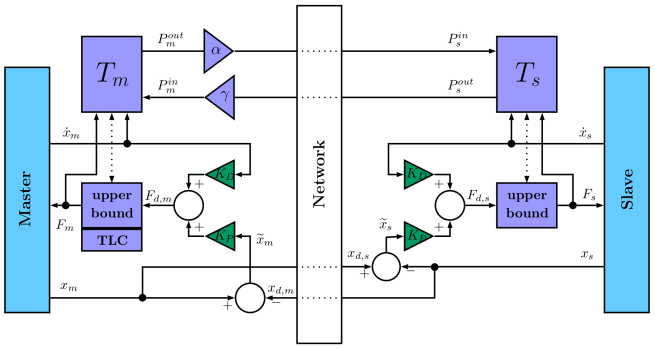

Fig. 1. Bilateral teleoperation architecture. The green blocks belong to the transparency layer, the violet blocks belong to the passivity layer. In the original two-layer architecture $\alpha = \gamma = 1$.

The controllers implemented within the *transparency layer* are PD controller

$$F_{d,i}(k) = K_{P,i}(x_i(k) - x_{d,i}(k)) + K_{D,i}\dot{x}_i(k) \quad (4)$$

where $F_{d,i}(k)$ is the desired command at time $t = kT_s$, T_s is sample time, $K_{P,i}$ and $K_{D,i}$ are the proportional and derivative gains, respectively; $x_i(k)$ is the current pose of the robot i whereas $x_{d,i}(k)$ is the desired pose equal to the pose of the robot at the other side of the network (i.e. $x_{d,m}(k) = x_s(k - d_{s2m}(k))$ where $d_{s2m}(k)$ is the slave-to-master delay at time k). The control parameters depend on the robot mechanics and they are tuned in order to obtain the best dynamic behavior.

The command $F_{d,i}$ requires a certain amount of energy to be actuated and such energy is provided by the energy tank T_i. It appears that for the same desired torque-velocity pair at the master and slave side, the needed energy is highly dependent on the manipulator's dynamics (1).

The mathematical model of the tank implemented within the *passivity layer* is

$$\begin{cases} \dot{x}_{t_i} = \dfrac{\sigma_i}{x_{t_i}} D_i(x) + \dfrac{1}{x_{t_i}}(\sigma_i P_i^{in} - P_i^{out}) + u_{t_i} \\ y_t = \dfrac{\partial T}{\partial x_t} = x_t \end{cases} \quad (5)$$

where $x_{t_i} \in \mathbb{R}$ is the state of the tank and $T_i(x_{t_i}) = \frac{1}{2}x_{t_i}^2$ is the energy stored in the tank. The tank can exchange energy through the power port $(u_{t_i}, y_{t_i}) \in \mathbb{R}\times\mathbb{R}$; $D_i(x_i) = \left(\frac{\partial H_i}{\partial x_i}\right)^T R_i(x_i)\frac{\partial H_i}{\partial x_i} \geq 0$ is the power dissipated by the system, and $P_i^{in} \geq 0$ and $P_i^{out} \geq 0$ are the incoming and outgoing power that a tank can exchange with the other tank. The desired control force $F_{d,i}$ provided by the transparency layer is implemented using the energy available in the tank T_i by interconnecting the power port $(F_i, \dot{x}_i)$ of the robot with the power port of the tank by

$$\begin{cases} F_i &= \dfrac{F_{d,i}}{x_{t_i}} y_{t_i} = \dfrac{F_{d,i}}{x_{t_i}} x_{t_i} = F_{d,i} \\ u_{t_i} &= -\dfrac{F_{d,i}^T}{x_{t_i}} \dot{x}_i \end{cases} \qquad i = m, s. \quad (6)$$

The following power balance holds

$$\dot{T}_i = \sigma_i D_i(x_i) + \sigma_i P_i^{in} - P_i^{out} + u_{t_i}^T y_t \quad (7)$$

which means that, if $\sigma_i = 1$ the tank stores the power dissipated by the robot $D_i(x_i)$ and the incoming power flow P_i^{in}, whereas the outgoing power flow P_i^{out} is released. Let $\bar{T}_i$ be the application-dependent upper bound on the capacity of the tanks, the policy used to set σ_i is:

$$\sigma_i = \begin{cases} 1, & \text{if } T_i(x_{t_i}) \leq \bar{T}_i \\ 0, & \text{otherwise.} \end{cases} \quad (8)$$

The energy can be injected into or extracted from the tank using the power port (u_{t_i}, y_{t_i}). To avoid singularities in (5) a minimum amount of energy ε_i must always be left in the tank, i.e. $T_i(x_{t_i}) \geq \varepsilon_i$, and the extraction of the energy from the tank is allowed only when the boolean σ_i^ε is equal to 1

$$\sigma_i^\varepsilon = \begin{cases} 1, & \text{if } T_i(x_{t_i}) \geq \varepsilon_i \\ 0, & \text{otherwise} \end{cases} \quad (9)$$

which means that the actual command is $\bar{F}_i = \sigma_i^\varepsilon F_i$. Anytime the tank level at the master side is smaller than T_m^{TLC}, the Tank Level Controller (TLC) injects a damping element at the master side to harvest energy from the user

$$\bar{F}_m = \sigma_m^\varepsilon F_m + F_m^{TLC}, \quad F_m^{TLC} = a(T_m(x_{t_m}) - T_m^{TLC})\dot{x}_m$$

where a is a positive constant; see [16] for more details.

There is also a mechanism to exchange energy between the two tanks: when the energy is below the threshold T_i^{req}, an *energy quantum* [16] is requested from the other tank

$$E_i^{req} = \begin{cases} 1, & \text{if } T_i(x_{t_i}) < T_i^{req} \\ 0, & \text{otherwise} \end{cases} \qquad i = m, s. \tag{10}$$

If the level of the tank at the other side is larger than the *availability* threshold T_i^{ava}, an *energy quantum* is sent

$$\beta_i = \begin{cases} 1, & \text{if } T_i(x_{t_i}) \geq T_i^{ava} \\ 0, & \text{otherwise.} \end{cases} \tag{11}$$

This mechanism helps to balance the energy level between the two tanks T_m and T_s. Furthermore, if the tank is already full, all the energy dissipated by the local robot is sent to the other side in order to not lose it. The energy transfer strategy is described by

$$\begin{cases} P_m^{out} = (1-\sigma_m)D_m + E_s^{req}\beta_m \bar{P}_m = P_s^{in} \\ P_s^{out} = (1-\sigma_s)D_s + E_m^{req}\beta_s \bar{P}_s = P_m^{in} \end{cases} \tag{12}$$

where the last equality holds when there is no communication delay. $\bar{P}_i > 0$ is the rate of energy flowing from one tank to the other and it is a design parameter. The bigger $\bar{P}_i$, the faster the energy transfer. All these thresholds are application-dependent and chosen to satisfy the inequalities: $\varepsilon_i < T_i^{req} < T_i^{ava} < \bar{T}_i$, for $i = m, s$.

In [17] it is proved that this teleoperation schema is passive with respect to the pair $\left((F_h, F_e), (\dot{x}_m, \dot{x}_s)\right)$.

III. Energy Scaling Factors

When dealing with manipulators characterized by similar dynamic models, performing the commanded task at the slave side will requires the same amount of energy supplied by the master side. When the involved manipulators are mechanically different this is no longer true. In Figure 2 we can see this behavior in our setup, which is described in Section IV, and where the slave is the higher energy demanding robot.

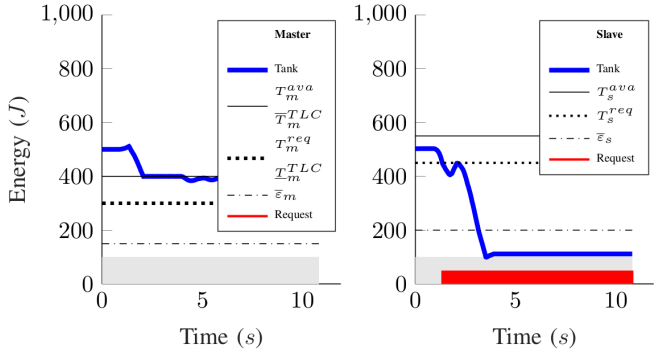

Fig. 2. Energy draining in the slave tank (right) due to mechanical mismatching between the master and slave robots.

When the robot dynamic models are available, a feasible solution would be to consider only the components of the force command needed to perform a certain movement and hide the compensation of all the mechanical factors within a dedicated inner model-based controller (i.e. inertia and friction). This paper aims to address this issue by scaling the energy that flows from/to the tanks at master and slave side in the passivity layer in order to meet the energy needs of the robots without an accurate mathematical model of the robots. We introduce two positive constants α and γ in the passivity layer in Figure 1, namely the *energy scaling factors*, such that:

$$\alpha\gamma = 1. \tag{13}$$

The original energy transfer protocol (12) becomes:

$$\begin{cases} \alpha P_m^{out} = \alpha\left((1-\sigma_m)D_m + E_s^{req}\beta_m \bar{P}_m\right) = P_s^{in} \\ \gamma P_s^{out} = \gamma\left((1-\sigma_s)D_s + E_m^{req}\beta_s \bar{P}_s\right) = P_m^{in}. \end{cases} \tag{14}$$

Loosely speaking, the power transmitted from the master is amplified by a factor α (> 1) and then stored in the tank of the slave side. The same happens for the power transmitted from the slave to the master, that is scaled down by a factor γ (< 1). We are now in a position to prove the main result of this paper.

Proposition 1: The scaling factors in the energy exchange protocol as shown in equation (14) preserves the passivity of the whole teleoperation system even if affected by communication delay.

Proof: Consider the total energy function

$$\begin{aligned} H(t) &= \alpha(H_m(t) + T_m(t)) + H_s(t) + T_s(t) + H_{ch}(t) \\ &= H_R(t) + H_{ch}(t) \end{aligned} \tag{15}$$

where $H_m(t)$ and $H_s(t)$ are the energy functions of the robots, $T_m(t)$ and $T_s(t)$ are the energy of the tanks and $H_{ch}(t)$ is the energy "stored" in the communication channel. Using (2) and (7), we obtain that

$$\begin{aligned} \dot{H}_R(t) = &- \alpha D_m(t) + \alpha F_m^T \dot{x}_m + \sigma_m \alpha D_m(t) + \alpha(\sigma_m P_m^{in} - \\ &- P_m^{out}) - D_s(t) + F_s^T \dot{x}_s + \sigma_s D_s(t) + (\sigma_s P_s^{in} \\ &- P_s^{out}) + \alpha u_{t_m} y_{t_m} + \alpha F_h^T \dot{x}_m + u_{t_s} y_{t_s} + F_e^T \dot{x}_s. \end{aligned}$$

Since the tanks and the robots are interconnected with the power preserving interconnection (6), we have that $F_i^T \dot{x}_i = -u_{t_i}^T y_{t_i}$, where $i = m, s$.

Substituting (14) and considering the time delay $\tau > 0$

$$\begin{aligned} \dot{H}_R(t) = &- (1-\sigma_m)\alpha D_m(t) - (1-\sigma_s)D_s(t) \\ &+ \sigma_m \alpha\gamma P_s^{out}(t-\tau) - \alpha P_m^{out}(t-\tau) + \\ &+ \sigma_s \alpha P_m^{out}(t-\tau) - P_s^{out}(t-\tau) \\ &+ \alpha F_h^T \dot{x}_m + F_e^T \dot{x}_s. \end{aligned} \tag{16}$$

According to Figure 1, the power flowing through the communication channel is given by:

$$\dot{H}_{ch}(t) = \alpha P_m^{out}(t) + P_s^{out}(t) - \alpha P_m^{out}(t-\tau) - P_s^{out}(t-\tau) \tag{17}$$

and, therefore, the energy stored in the communication channel is represented by the following positive storage function

$$H_{ch}(t) = \int_{t-\tau}^{t} \left(\alpha P_m^{out}(\rho) + P_s^{out}(\rho)\right) d\rho.$$

Fig. 3. Master device.

Fig. 4. Slave device.

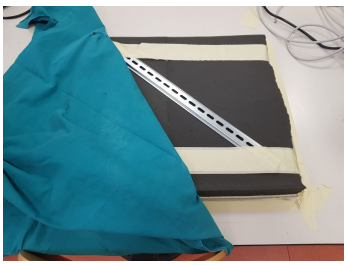

Fig. 5. Environment

Considering that $\sigma_m, \sigma_s \in \{0, 1\}$ and combining (16) with (17) we obtain the following power balance:

$$\dot{H}(t) \leq (\sigma_m - 1)P_s^{out}(t-\tau) + (\sigma_s - 1)\alpha P_m^{out}(t-\tau) + \\ + \alpha F_h^T \dot{x}_m + F_e^T \dot{x}_s \leq \alpha F_h^T \dot{x}_m + F_e^T \dot{x}_s$$

which proves the passivity of the overall teleoperation system with respect to the two power ports $(F_e, \dot{x}_s)$ and $(F_h, \alpha\dot{x}_m)$.

The same proof could be done considering the energy function

$$H(t) = H_m(t) + T_m(t) + \gamma(H_s(t) + T_s(t)) + H_{ch}(t)$$

instead of (15). ■

It is worth noting that the scaling factors allows to prove the passivity with respect to a scaled power. Nevertheless, this is sufficient for guaranteeing a safe behavior when interacting with passive environments. The parameter α (and so γ) is application-dependent and is tuned on the real system: as a rule of thumb, for low motion as in the present case, this parameter could be chosen as the ratio between the proportional gains $K_{P,m}$, $K_{P,s}$.

IV. Experimental Setup

The experimental setup is designed following the requirements highlighted in [5]. The goal of the master device is to allow sonographers to perform the procedure in the remote environment as they were next to the patient. They have to tele-control the ultrasound probe at the slave side and to perceive the interaction with the patient. We use the haptic 3D Systems TOUCH™ [18] as input device rendering force feedback on 3-DoF (Fig. 3). At the slave side we use a Barrett WAM™ robot [19]. On this manipulator, an ultrasound probe is mounted at the end-effector (Fig. 4).

These devices have very different mechanical characteristics and their dynamic models are not fully available in the distributed APIs. For these reasons, the energy scaling factor is a feasible solution to provide an effective system for tele-echography.

We will validate the proposed architecture in three types of working conditions:

- free motion: the slave manipulator is moved freely without interacting with the environment;
- soft contact: the US probe gets in contact with a sponge;
- hard contact: the US probe gets in contact with a metal bar above the sponge. Figure 5 shows this setup.

An ATI Mini force sensor is located between the last active joint of the WAM arm and the US probe. This sensor provides direct measurements of the interaction force/torque. Such measurements are used in our setup as a ground-truth and will be eventually integrated in the control architecture in the future. The force feedback provided by the TOUCH haptic device to the user is estimated by its API using motor currents.

V. Experimental Results

The effectiveness of a Tele-Echography system is given by its level of transparency and stability. The contact experiments are characterized by an initial interaction with the sponge (soft contact) and then by an interaction with the metal bar above the sponge (hard contact).

The teleoperation system has to guarantee stability during both free motion and interaction with the environment, and with/without communication delay. For each experiment, we choose a large delay to demonstrate that the proposed algorithm detects critical situations (i.e. the energy level within the tank is getting closer to the threshold) and maintains the system stability by enforcing passive behaviors.

The experiments are presented in each figure by showing master/slave positions, orientations, forces and energy tank levels. The energy tank plots include the thresholds $\varepsilon_i, T_i^{req}, T_i^{ava}, T_m^{TLC}$ explained in Section II. Any time an energy request is sent ($E_i^{req} = 1$ in (10)), a red spike is drawn at the bottom of the plots related to T_m and T_s.

The On/Off condition (9) for cutting the commands and activating the TLC produces chattering. In order to make the behavior of the system smoother we introduce a hysteresis mechanism that depends also on the value at the previous time instant $k-1$. For the new $\bar{\sigma}_i^{\varepsilon}$ we have an upper and lower pair $\underline{\varepsilon}_i, \overline{\varepsilon}_i$ such that

$$\bar{\sigma}_i^{\varepsilon}(k) = \begin{cases} 1, & \text{if } T_i(k) \geq \underline{\varepsilon}_i \text{ or} \\ & (T_i(k) \in (\underline{\varepsilon}_i, \overline{\varepsilon}_i] \text{ and } \bar{\sigma}_i^{\varepsilon}(k-1) == 1) \\ 0, & \text{if } T_i(k) \leq \underline{\varepsilon}_i \text{ or} \\ & (T_i(k) \in (\underline{\varepsilon}_i, \overline{\varepsilon}_i] \text{ and } \bar{\sigma}_i^{\varepsilon}(k-1) == 0). \end{cases}$$

A similar condition holds for the TLC with the thresholds $\underline{T}_i^{TLC}, \overline{T}_i^{TLC}$.

In the force plots, the master forces are scaled in order to make possible the comparison with the slave forces. The scaling factor is given roughly by the ratio between the proportional gains of the master/slave controllers, $K_{P,m}$ and $K_{P,s}$, in (4). In fact the contribution of the derivative

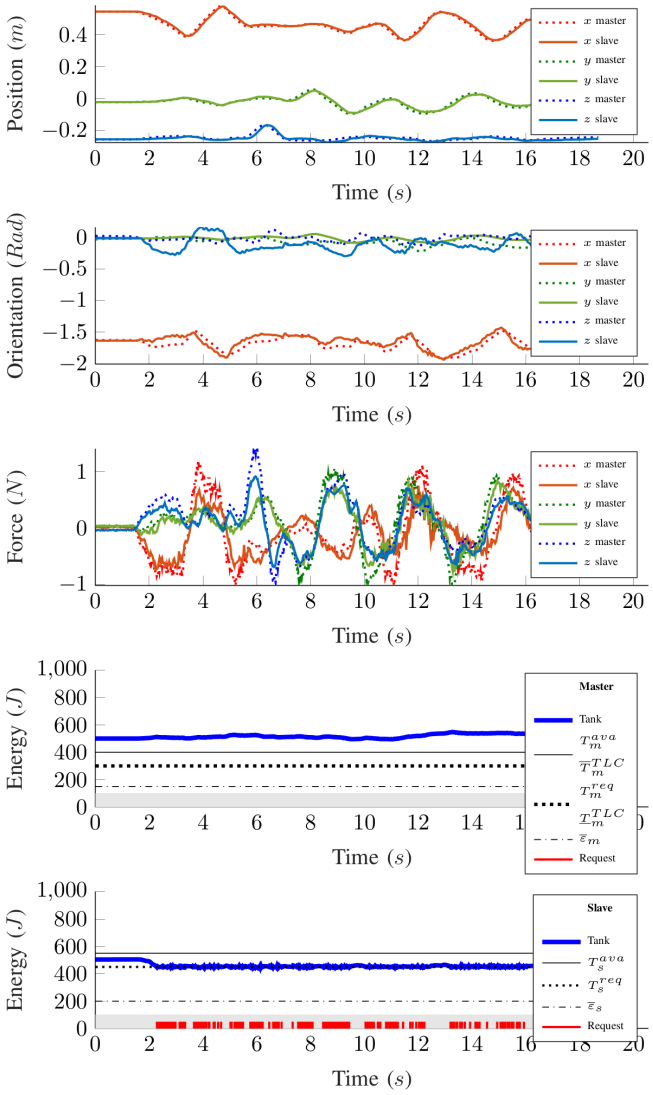

Fig. 6. Free motion experiment without communication delay.

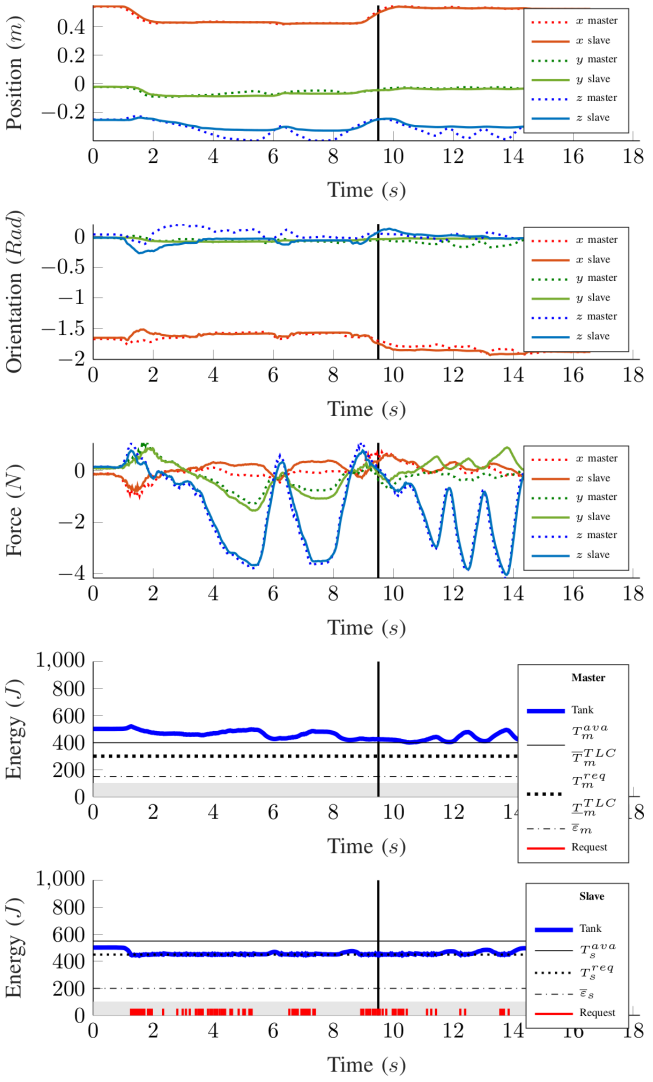

Fig. 7. Contact experiment without communication delay.

gains could be ignored because the velocity over the tele-echography task is low.

We now discuss stability and performance in the different working conditions.

1) Free motion without delay: The experiment consists of a translational movement that has a non-zero component on each axes. The communication channel of the system is not affected by delay. The feedback forces are not due to interaction: the operator perceives the slave manipulator inertia due to the master-slave position error required by the PD controller to generate command torque sufficient to move the robot. Figure 6 shows that the energies stored in the tanks stay around an equilibrium point since the slave side reacts promptly to the master commands. The position tracking error is very low, whereas some errors can be seen in the orientation. Such tracking errors are meanly due to the friction that the PD controller of the wrist is not able to compensate properly.

2) Contact without delay: In this experiment the US probe at the slave end-effector interacts initially with the sponge and then with the metal bar (the vertical line indicates the transition time). The energies in the tanks shown in Figure 7 remain around an equilibrium point since, without delay, an interaction with a passive environment does not create unstable behaviors. It worth highlighting that the thresholds T_i^{req}, T_i^{ava} are not equal for the slave robot and the master robot due to the different dynamics.

3) Free motion with delay: The slave robot is now moving freely but the communication channel is affected by a large delay. The operator performs some fast movements that, combined with the delay, bring the system close to instability. The result is an energy draining in the tanks as shown in Figure 8; in particular, the slave tank goes below the minimum threshold $\underline{\varepsilon}_s$ preventing the slave manipulator to execute further commands. The system could be reactivated by harvesting energy at the master side using the TLC mechanism. In this experiment, the two-layer algorithm

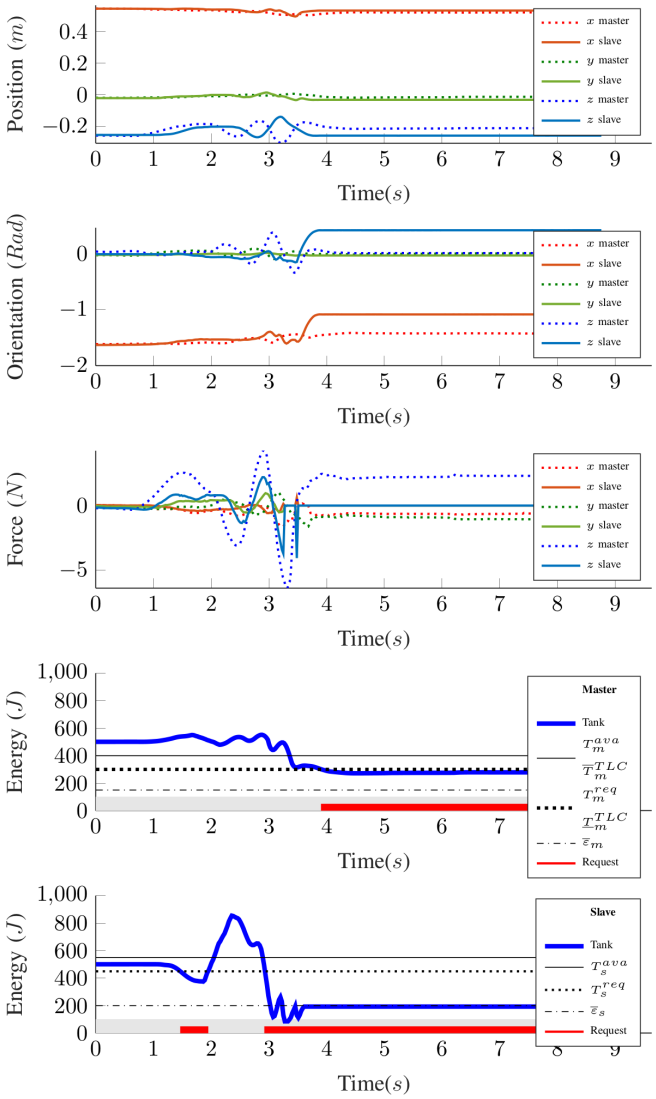

Fig. 8. Free motion experiment with a communication delay equal to $0.2s$ from slave-to-master and $0.2s$ from master-to-slave.

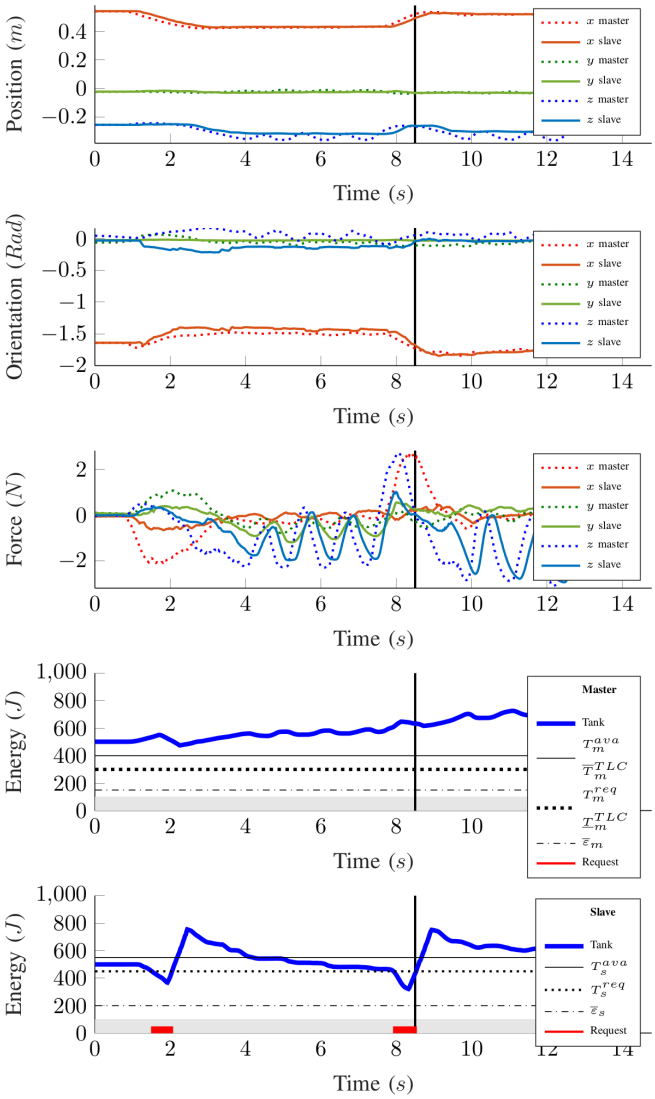

Fig. 9. Contact experiment with a communication delay equal to $0.2s$ from slave-to-master and $0.2s$ from master-to-slave.

avoids unstable behaviors as expected. The role of the scaling factor proposed in this paper is not to prevent the action of the passivity layer but to activate it only when it is really necessary. This fact can be appreciated by comparing Figure 8 with Figure 2 where the draining of the energy in the tanks is much faster.

4) Contact with delay: In this case the teleoperation system has to deal with the same communication delay (round-trip-time delay equal to $0.4s$) as in the previous case. The interaction with a passive environment (as the sponge is, also with the bar above) makes the overall system stable without the critical situations seen in Figure 8. Such "passifying" behavior can be appreciated in Figure 9. The *saw-tooth*-like evolution of the energy level within the slave tank T_s is due to the "temporal disalignment" between the energy request (when the request threshold T_s^{req} is crossed) and the moment the energy is actually received. Communication delays affect the shape of such saw-tooth behavior. A possible solution to overcome this oscillatory behavior would be to introduce a maximum value for the requested energy. Figure 9 shows that the displacement between the master position and the slave position is mainly along the z axis, the axis along which the probe is interacting with the environment.

VI. Conclusions

Tele-Echography systems may solve the problem of lack of skilled sonographers available in remote or scarcely populated areas. Since in this type of systems the slave robot and the master haptic device are mechanically different we propose an energy scaling factor mechanism that preserves the passivity of a two-layer bilateral architecture. This allows the implementation of a wide range of control strategy without requiring the accurate model of the robots but just a rough estimation of the ratio of their inertia. The experiments carried out with our full Tele-Echography setup show the effectiveness of this approach even in case of communication delays.

REFERENCES

[1] A. Gourdon, P. Poignet, G. Poisson, P. Vieyres, and P. Marche, "A new robotic mechanism for medical application," in *Advanced Intelligent Mechatronics, 1999. Proceedings. 1999 IEEE/ASME International Conference on*. IEEE, 1999, pp. 33–38.

[2] A. V. Gonzales, P. Cinquin, J. Troccaz, A. Guerraz, B. Hennion, F. Pellissier, P. Thorel, F. Courreges, A. Gourdon, G. Poisson, and Others, "TER: a system for robotic tele-echography," in *International Conference on Medical Image Computing and Computer-Assisted Intervention*. Springer, 2001, pp. 326–334.

[3] J. J. Banihachemi, E. Boidard, J. L. Bosson, L. Bressollette, I. Bricault, P. Cinquin, G. Ferretti, M. Marchal, T. Martinelli, A. Moreau-Gaudry, F. Pellissier, C. Roux, D. Saragaglia, P. Thorel, J. Troccaz, and A. Vilchis, *The tele-echography robot: A robot for remote ultrasonic examination*. Berlin, Heidelberg: Springer Berlin Heidelberg, 2008, pp. 91–99. [Online]. Available: https://doi.org/10.1007/978-3-540-72999-0_7

[4] P. Chatelain, A. Krupa, and N. Navab, "Confidence-driven control of an ultrasound probe," *IEEE Transactions on Robotics*, vol. 33, no. 6, pp. 1410–1424, 2017.

[5] K. Mathiassen, J. E. Fjellin, K. Glette, P. K. Hol, and O. J. Elle, "An Ultrasound Robotic System Using the Commercial Robot UR5," *Frontiers in Robotics and AI*, vol. 3, no. February, pp. 1–16, 2016. [Online]. Available: http://journal.frontiersin.org/Article/10.3389/frobt.2016.00001/abstract

[6] D. A. Lawrence, "Stability and Transparency in Bilateral Teleoperation," *IEEE Transactions on Robotics and Automation*, vol. 9, no. 5, pp. 624–637, 1993.

[7] N. Hogan, "Controlling impedance at the man/machine interface," in *Proceedings, 1989 International Conference on Robotics and Automation*, May 1989, pp. 1626–1631 vol.3.

[8] A. v. d. Schaft and A. J. Schaft, *L2-Gain and Passivity in Nonlinear Control*, 2nd ed. Berlin, Heidelberg: Springer-Verlag, 1999.

[9] D. Lee and M. W. Spong, "Passive bilateral teleoperation with constant time delay," *Robotics, IEEE Transactions on*, vol. 22, no. 2, pp. 269–281, 2006.

[10] N. Chopra, M. W. Spong, and R. Lozano, "Synchronization of bilateral teleoperators with time delay," *Automatica*, vol. 44, no. 8, pp. 2142–2148, 2008.

[11] J.-H. Ryu, J. Artigas, and C. Preusche, "A passive bilateral control scheme for a teleoperator with time-varying communication delay," *Mechatronics*, vol. 20, no. 7, pp. 812–823, 2010.

[12] D. Lee and K. Huang, "Passive-set-position-modulation framework for interactive robotic systems," *Robotics, IEEE Transactions on*, vol. 26, no. 2, pp. 354–369, 2010.

[13] P. F. Hokayem and M. W. Spong, "Bilateral teleoperation: An historical survey," *Automatica*, vol. 42, no. 12, pp. 2035–2057, 2006.

[14] E. Nuño, L. Basañez, and R. Ortega, "Passivity-based control for bilateral teleoperation: A tutorial," *Automatica*, vol. 47, no. 3, pp. 485–495, 2011.

[15] R. Muradore and P. Fiorini, "A review of bilateral teleoperation algorithms," *Acta Polytechnica Hungarica*, vol. 13, no. 1, pp. 191–208, 2016.

[16] M. Franken, S. Stramigioli, S. Misra, C. Secchi, and A. Macchelli, "Bilateral telemanipulation with time delays: A two-layer approach combining passivity and transparency," *IEEE Transactions on Robotics*, vol. 27, no. 4, pp. 741–756, Aug 2011.

[17] F. Ferraguti, N. Preda, A. Manurung, M. Bonf, O. Lambercy, R. Gassert, R. Muradore, P. Fiorini, and C. Secchi, "An energy tank-based interactive control architecture for autonomous and teleoperated robotic surgery," *IEEE Transactions on Robotics*, vol. 31, no. 5, pp. 1073–1088, Oct 2015.

[18] "3Dsystems Touch haptic device," https://it.3dsystems.com/haptics-devices/touch.

[19] "The WAM^{TM}Arm," https://www.barrett.com/wam-arm.